inter•noise 96
25th Anniversary Congress – Liverpool

INCE: 43

NEW DEVELOPMENTS IN EXPERIMENTAL SPATIAL POWER FLOW

J D Blotter, D H Coe, R L West & L D Mitchell

Mechanical Engineering Department, Virginia Polytechnic Institute & State University, Blacksburg, Virginia 24061-0238, USA

1. INTRODUCTION

This paper discusses new developments in the Experimental Spatial Power Flow (ESPF) method. The ESPF approach retains the spatial representation of the power flow, obtained from analytical models, and represents the actual boundary conditions by using experimental data obtained from a scanning laser Doppler Vibrometer (SLDV) [1]. This paper will demonstrate that the ESPF method satisfies the conservation of energy principle, in that, power injected to a simply supported plate from an external source is shown to compare with the power flow computed by the ESPF method. The simply supported plate is excited by two shakers which are placed diagonally across the plate. The power injected to the plate is computed from impedance head measurements at the two shaker locations. This injected power measurement is then compared to the results obtained from the ESPF method.

2. BACKGROUND

The concept behind power-flow methods is that the magnitudes and locations of the energy sources and sinks, as well as the paths of energy transmission, can be determined in vibrating structures. The difficulties associated with many of the power-flow techniques presently developed, stem primarily from two issues. The first issue is that a spatial model of the structure's dynamic response is required to map the energy path in the structure. Secondly, it is extremely difficult to analytically model the actual boundary conditions and geometry of the test structure. Analytical models provide a spatial representation of the response but accurate modeling of the actual boundary conditions on the structure are unknown both in magnitude and representation. Experimental models inherently include the actual boundary conditions in the measurements of the dynamic response but do not typically develop an adequate spatial model of the response.

The Experimental Spatial Power Flow (ESPF) method discussed in this paper provides a spatially continuous power-flow model which inherently includes the actual boundary conditions since it is derived from experimental measurements [1][2]. The ESPF method is developed around the high spatial density measurement capability of a scanning laser Doppler vibrometer (SLDV). The spatially dense measurements acquired by the SLDV are used to solve for a spatially continuous 3-D complex-valued representation of the velocity field over the structure [3]. This velocity field is integrated in time to obtain the continuous 3-D complex-valued displacement field. From this representation of the displacement field the generalized forces are determined [3].

In plates, power flow due to transverse motion only, is comprised of three generalized forces and velocities. The generalized forces are the bending moments M_x, M_y, twisting moments M_{xy}, M_{yx}, and the shear forces Q_x, Q_y. Using Love-Kirchoff plate theory, these components can be expressed in terms of spatial derivatives of the transverse displacement field w.The generalized velocities which correspond to these generalized forces are the angular velocities $\dot{\theta}_x, \dot{\theta}_y$, and the transverse velocity $\dot{w}$. Using this notation the power flow can be expressed as shown by Eqs. 1 and 2, where the asterisk represents the complex conjugate [4].

$$q_x = \mathrm{Re}\left[Q_x\dot{w}^* + M_x\dot{\theta}_y^* - M_{xy}\dot{\theta}_x^*\right] \quad (1)$$

$$q_y = \mathrm{Re}\left[Q_y\dot{w}^* - M_y\dot{\theta}_x^* + M_{yx}\dot{\theta}_y^*\right] \quad (2)$$

3. EXPERIMENTAL SETUP

The ESPF approach was applied to a 380.0 mm x 300.0 mm x 1.6 mm steel plate. The plate had a Young's modulus of elasticity of 2.04E11 Pa, structural damping factor of 0.001, and Poisson's ratio of 0.29. The test plate was mounted to a rigid steel frame by thin steel shims as shown by Fig. 1. Five screws equally spaced along each edge of the plate were used to attach the plate to the shims. The test structure was designed to simulate a simply supported plate. However, this assumption is not made or required in any part of this experimental procedure, as the boundary conditions are inherently modeled in the solution based on the laser data.

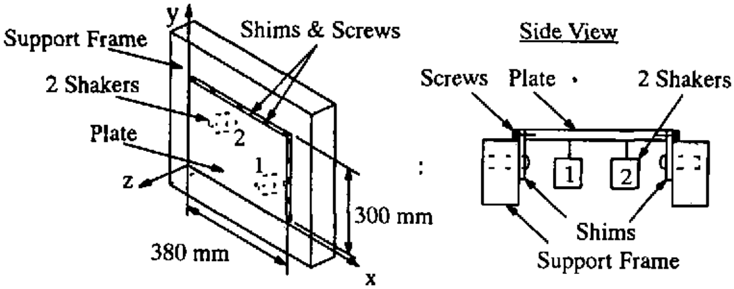

FIGURE 1. SIMPLY SUPPORTED PLATE SETUP

The steel plate was harmonically excited with two electromagnetic shakers. The shakers were hung from bungee cords and connected to impedance heads. The impedance heads were connected to the plate through 2.0 cm diameter mount plates which were glued to the plate. Shaker 1, was attached to the plate at x=290.0 mm, y=90.0 mm. Shaker 2 was attached at x=90.0 mm, y=210.0 mm.

4. EXPERIMENTAL RESULTS

79.0 Hz Case

In the 79.0 Hz case the two shakers were phased such that shaker 2, as indicated in Fig. 1, lagged shaker 1 by 174.62 degrees and had a magnitude of 89% of shaker 1. Figure 2 illustrates the power flow in the plate computed by the ESPF method. The magnitude of the velocity field indicating the operating shape of the plate is also superimposed on the power flow vector plot. The darker areas represent points of high velocity. The 2 large black dots on the plate represent the relative size and location of the shaker and impedance head mount plates while the small black dots on the border represent the screw locations as discussed in the experimental setup. The ring around the first shaker indicates the control volume where the maximum power flow occurs.

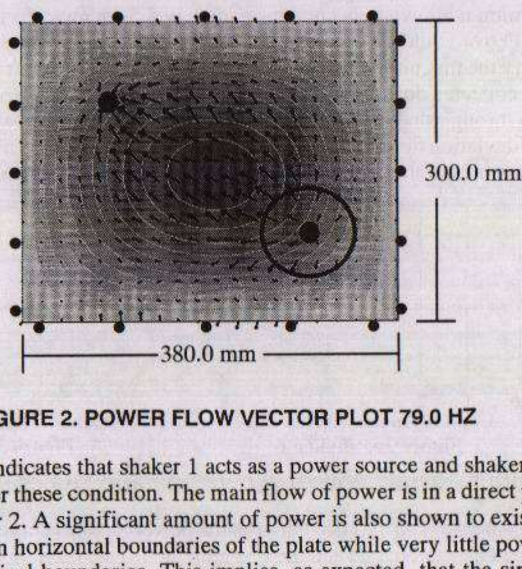

FIGURE 2. POWER FLOW VECTOR PLOT 79.0 HZ

Figure 2 clearly indicates that shaker 1 acts as a power source and shaker 2 acts as a power sink under these condition. The main flow of power is in a direct path from shaker 1 to shaker 2. A significant amount of power is also shown to exist on both the top and bottom horizontal boundaries of the plate while very little power is detected on the vertical boundaries. This implies, as expected, that the simply supported boundary conditions are not perfect.

Under ideal point force conditions the largest power flow vectors would exist at the point source and then decrease in magnitude due to various loss mechanisms as the distance from the source is increased. In this case, with the 2.0 cm diameter mount plates, the maximum power flow should occur at a radius of 1.0 cm from the center of the mount plate. Figure 2 indicates that the largest vectors are shown to occur slightly further than 1.0 cm away from the center of the mount plates.

To further investigate this concern, the net power crossing a circular control volume, centered at the source, was computed. The control volume was then incrementally enlarged in the radial direction and the net power flow was again computed. The net power flow normal to each circular control volume was computed at 72 equally spaced points around each control volume. These 72 points were then used to compute the total power normal to the control volume. The total power in 40 control volumes at radial increments of 0.2 cm were computed for a total radial distance of 8.0 cm from the center of the mount plate.

Figures 3a and 3b show plots of the net power flow crossing each circular control volume for the first 30 control volumes. Figure 3a illustrates that the maximum power flow of 0.28 watts was obtained at a radial distance of 5.0 cm from the center of the source. This is 4.0 cm away from where the maximum power flow should theoretically occur. In this power flow model an 8x8 uniform quintic B-spline mesh was used to represent the velocity field. Using a more refined mesh around the locations of the source and sink would decrease the radius at which the maximum power flow was obtained and improve the accuracy. There is also some error due to the discrete integration performed to obtain the total power flow crossing each control volume. Figure 3b illustrates the decline in power flow as it leaves through shaker 2. The maximum is shown to occur approximately 5.5 cm away from the sink. Again, this spatial error could be decreased by increasing the mesh density of the model.

To verify the magnitudes of the power flow, time series data from the impedance heads was collected during the laser scanning process. The mean power injected into the system through shaker 1 computed from the impedance head was 0.25 watts with a standard deviation of 0.00027 watts. The mean power leaving through shaker 2 was computed as 0.24 watts with a standard deviation of 0.00034 watts.

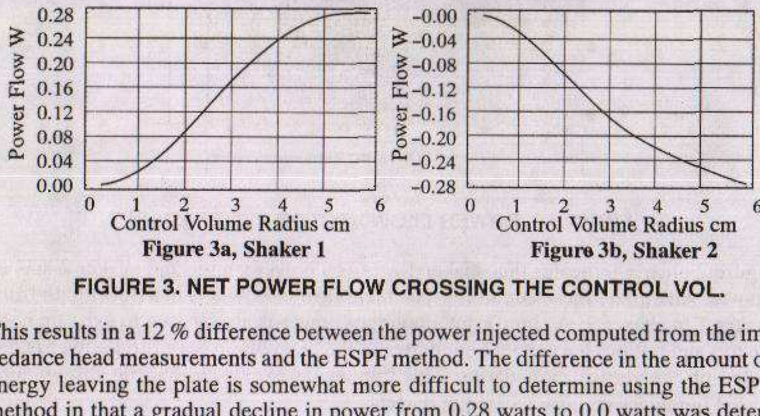

Figure 3a, Shaker 1 **Figure 3b, Shaker 2**

FIGURE 3. NET POWER FLOW CROSSING THE CONTROL VOL.

This results in a 12 % difference between the power injected computed from the impedance head measurements and the ESPF method. The difference in the amount of energy leaving the plate is somewhat more difficult to determine using the ESPF method in that a gradual decline in power from 0.28 watts to 0.0 watts was determined. Although these are significant percentages, the results are still promising based on several reasons. The first is that the calibration constants for the impedance heads had large variations and were determined to be sensitive to torque. Slight laser calibration error could also account for some of the difference between the results. Other factors such as uncertainty in the plate dimensions, material properties, and misalignment in the force locations could also affect the results. Considering these possible experimental errors it was concluded that the ESPF method was able to conserve energy.

The power entering and leaving the plate were calculated to be nearly the same value. This is due to the relatively large amount of power traveling through the plate as compared to the losses.

311.0 Hz Case

In the 311.0 Hz case the two shakers were phased such that shaker 2 lagged shaker 1 by 174.57 degrees and had a magnitude of 85% of shaker 1. Figure 4 illustrates that the power flow for this case is not a direct flow from shaker 1 to shaker 2. The main power flow path is shown to be in an "L" shaped pattern starting at shaker 1, flowing in the negative x direction and then in the positive y direction. A relatively weaker power flow path is also shown to exist which first leaves shaker 1 flowing in a positive y direction and then in a negative x direction. Very little power flow through the center of the plate is detected. The operating shape illustrates that 311.0 Hz corresponds to a frequency between the 2x1 and the 1x2 modes of the plate. Again, as in the 79.0 Hz case, the top and bottom horizontal boundaries show significant power flow magnitudes compared to the vertical boundaries.

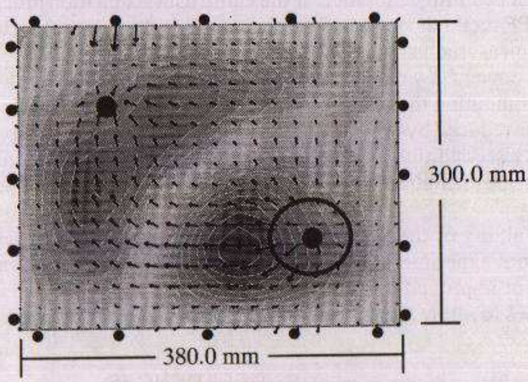

FIGURE 4. POWER FLOW VECTOR PLOT 311.0 HZ

Figures 5a and 5b indicate that the maximum power flow injected into the plate computed by the ESPF method occurred at a radial distance of 4.5 cm from the center of the source. The spatial error of where the maximum power flow occurs is again due to the 8x8 quintic B-spline mesh and could be reduced by mesh refinement. The maximum magnitude was 1.40 mW. The power injected into the plate computed from the impedance head measurements was 1.42 mW with a standard deviation of 7.0E−3 mW. This results in a difference of 1.4% which is significantly lower than the first case of 79.0 Hz. This is partially due to the fact that the amount of experimental error due to calibration of the electronic system used in the data acquisition was reduced.

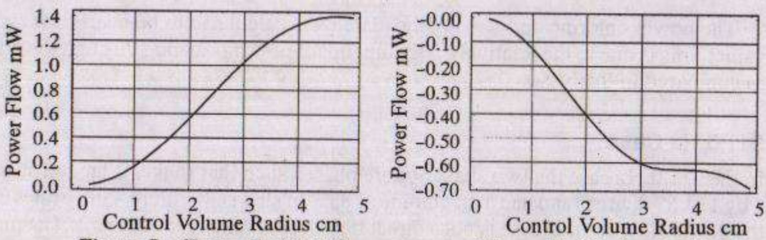

Figure 5a, Shaker 1, 311.0 Hz **Figure 5b, Shaker 2, 311.0 Hz**

FIGURE 5. NET POWER FLOW CROSSING CONTROL VOL.

5. SUMMARY

In summary it can be concluded that the ESPF method can predict the magnitude of the power flow to within 12% as indicated by the results from the 79.0 Hz case. However, after careful calibration of the entire data acquisition process it was shown that the ESPF method computed the magnitude of the power flow to within 1.4% of the power measured using an impedance head.

The power flow results also indicated that a spatial error of 4.0 cm was obtained when computing the exact location of the maximum power flow. This spatial error could be reduced by mesh refinement but will not be completely removed. However, in most test conditions, when structures are large compared to the points of excitation or when the excitation is more of a distributed load this spatial error will be insignificant.

The ability of the ESPF method to extract a spatial representation of the power flow from experimental data has been validated. Further research in this area will consist of improved calibration techniques and the implementation of non-uniform B-splines to allow local mesh refinement in the areas of concentrated loads

6. REFERENCES

[1] Blotter, J. D. and West, R. L., "Identification Of Energy Sources And Sinks In Plates By Means Of A Scanning Laser Doppler Vibrometer", *Noise Control Engineering Journal,* Vol. 44, No. 2, 1996, pp. 61-68.

[2] Blotter, J. D., and West, R. L., "Experimental And Analytical Power Flow In Beams Using A Scanning Laser Doppler Vibrometer", *J. of Shock and Vibration,* Accepted Oct. 1995.

[3] Montgomery, D. E., West, R. L, and P. P. H. Nguyen, P. P. H., "Modeling of 3-D Velocity Response Fields Using a Least-Squares Discrete Finite Element Formulation", *Proceedings of the 12th International Modal Analysis Conference,* Vol. 2, 1994, pp. 926-932.

[4] Noiseux, D. U., "Measurement Of Power Flow In Uniform Beams And Plates", *J. of the Acoust. Soc. of Am.,* 47(1), Part 2, 1970, pp. 238-247.